Date of publication xxxx 00, 0000, date of current version xxxx 00, 0000.

Digital Object Identifier 10.1109/ACCESS.2017.DOI

On the Application of Directional Antennas in Multi-tier Unmanned Aerial Vehicle Networks

JING ZHANG[1], (Member, IEEE), HUAN XU[1], LIN XIANG[2], (Member, IEEE), AND JUN YANG.[3]

[1]School of Electronic Information and Communications, Huazhong University of Science and Technology, Wuhan 430074, Hubei, China (emails: {zhangjing, xuhuan1995}@hust.edu.cn)

[2]Interdisciplinary Centre for Security, Reliability and Trust (SnT), University of Luxembourg, L-1855 Luxembourg, Luxembourg (email: lin.xiang@uni.lu)

[3]School of Computer Science and Technology, Huazhong University of Science and Technology, Wuhan 430074, China (email: junyang_cs@hust.edu.cn)

Corresponding author: Jun Yang (e-mail: junyang_cs@hust.edu.cn).

This work was supported in part by the Ministry of Science and Technology of China under Grant 2016YFE0119000, in part by the European Research Council (ERC) project AGNOSTIC.

ABSTRACT This paper evaluates the performance of downlink information transmission in three-dimensional (3D) unmanned aerial vehicle (UAV) networks, where multi-tier UAVs of different types and flying altitudes employ directional antennas for communication with ground user equipments (UEs). We introduce a novel tractable antenna gain model, which is a nonlinear function of the elevation angle and the directivity factor, for directional antenna-based UAV communication. Since the transmission range of a UAV is limited by its antenna gain and the receiving threshold of the UEs, only UAVs located in a finite region in each tier can successfully communicate with the UEs. The communication connectivity, association probability as well as coverage probability of the considered multi-tier UAV networks are derived for both line-of-sight (LoS) and non-line-of-sight (NLoS) propagation scenarios. Our analytical results unveil that, for UAV networks employing directional antennas, a necessary tradeoff between connectivity and coverage probability exists. Consequently, UAVs flying at low altitudes require a large elevation angle in order to successfully serve the ground UEs. Moreover, by employing directional antennas an optimal directivity factor exists for maximizing the coverage probability of the multi-tier UAV networks. Simulation results validate the analytical derivations and suggest the application of high-gain directional antennas to improve downlink transmission in the multi-tier UAV networks.

INDEX TERMS directional antenna, multi-tier network, stochastic geometry, Unmanned aerial vehicle (UAV).

I. INTRODUCTION

Unmanned aerial vehicles (UAVs) have gained increasing interest in both academia [1], [2] and industry [3], [4]. By flying in the sky at moderate to high speeds, UAVs can provide flexible short-term services such as information collection over wireless, traffic surveillance, and disaster information dissemination to wherever demand occurs at a low cost [5]. An energy-efficient data collection method was proposed for UAV-aided networks in [6], which can ensure fairness for ground sensors. For surveillance of multi-domain Internet-of-Things (IoT) devices, an approach based on linear integer programming was proposed in [7] to minimize the maximum flying range of UAVs. In [8], joint optimization of the trajectory and scheduling of UAVs was investigated for a UAV-assisted emergency network, where UAVs are deployed to re-establish communication between ground devices and surviving BSs in the aftermath of natural disasters. Exploiting the highly flexible and low-cost deployment of UAVs, several works have suggested employing UAVs as aerial base stations (ABSs) to serve ground user equipments (UEs) directly and offload traffic for terrestrial cellular networks. A novel three-dimensional (3D) ABS deployment was investigated in [9] for maximizing the number of UEs within ABSs' coverage while fulfilling the quality-of-service (QoS) requirements of UEs. The performance of a two-tier network consisting of ABSs and terrestrial cellular base stations (BSs) was analyzed in [10], where ABSs are deployed to offload cellular traffic in hotspot areas. A distributed algorithm was further proposed to minimize the average distance between UAVs

and UEs without degrading the communication between UAVs and cellular BSs [11].

The existing works [9]–[11] have considered omni-directional antennas for UAV communication. However, as omni-directional antennas employ uniform antenna gains in all directions, the performance of UAV communication is severely limited due to excess interference from neighboring UAVs and terrestrial nodes, especially at high altitudes with abundant line-of-sight (LoS) propagation [4]. To tackle this issue, application of directional antennas for efficient UAV communications has recently gained tremendous attention due to the associated advantages of enhanced signal transmission, interference mitigation, and payload deployment. In particular, different from omni-directional antennas, UAV with directional antenna generates highly directive beams with strengthened signal power in the main lobe and reduced power leakage in the side lobes. Consequently, directional antennas with high antenna gain can improve the communication distance and the data rate in the downlink transmission without increasing the power consumption of the UAVs. Moreover, due to the small footprint, the interference to other UAVs and the terrestrial cellular system is reduced by employing directional antenna. The resulting interference mitigation capability can significantly enhance the performance of UAV networks. Furthermore, due to the size, weight, and power (SWAP) constraints of UAVs, an on-board deployment of large-scale antenna array is usually difficult, whereas directional antennas with large antenna gain and flexible payload deployment provide a promising alternative for UAVs. Considering directional antennas in UAV networks, joint optimization of UAVs' flying altitude and antenna beamwidth was investigated in [12] for maximizing the throughput of downlink multicasting, downlink broadcasting, and uplink multiple access, respectively. A long-range broadband aerial communication system using directional antennas was proposed in [13], where a Wi-Fi infrastructure established in the air is exploited for real-time communication. Directional antenna has also been combined with millimeter-wave technique, for high-resolution 3D localization in [14], where multi-level beamforming with compressive sensing based channel estimation is usually employed [15], [16].

Motivated by its huge potential, this paper investigates the application of directional antenna in UAV networks with a focus on evaluating the network performance in the downlink. Different from terrestrial cellular networks, UAV network occupies a range of altitudes in the air and inherently has a 3D network topology. This is usually captured by a multi-tier network model for performance evaluation, where UAVs of a given tier keep flying at a certain altitude while communicating with the ground UEs. Considering a multi-tier UAV network deployed atop terrestrial heterogeneous networks (HetNets), a cell management framework was proposed in [17] to improve the communication coverage and retransmission time for UEs in congested networks. In [18], the authors investigated the spectral efficiency of downlink multi-tier UAV networks and derived the optimal intensities and altitudes for UAVs in different tiers. Assuming omni-directional antennas, the association probability, successful transmission probability, and area spectral efficiency of multi-tier UAV networks were analyzed in [19]. Despite the fruitful development in the aforementioned works [17]–[19], a comprehensive performance evaluation for multi-tier UAV wireless networks employing directional antennas is still lacking, which may be hindered by two potential challenges. In particular, in the existing literature, especially for millimeter-wave communication, the gain of directional antenna was usually modeled as a flat-top antenna pattern with the maximum antenna gain attained in the main lobe [20]. Although this model is suitable for receivers at fixed location and within short transmission distance, it is not applicable for UAV communication networks. This is becauce the UAV flying in the sky usually changes its position and hence, the angle of arrival (AoA) and angle of departure (AoD), which will impact the antenna gain. In this case, the antenna gain model should capture the complicated channel variations associated with UAV communications along its flying trajectory, including channel conditions both line-of-sight (LoS) and non-line-of-sight (NLoS) propagation. Therefore, a novel tractable antenna gain model should be introduced for UAV communication networks.

On the other hand, the battery-powered UAVs usually suffer from severely limited energy supply. To reduce energy consumption and prolong the lifetime, signal transmission at UAVs has to respect a maximum transmit power budget and, at the same time, ensure at least a minimum receiving power at the ground UEs required to activate the receiving circuits. Therefore, transmit power management at different flying heights is crucial for UAVs and has been extensively studied in the literature while assuming omni-directional antennas [21]–[23]. In [21], optimal power control for UAV-assisted networks serving underlaying D2D communication was investigated for minimizing the energy consumption and increasing the battery's service time. In space-air-ground three-tier HetNets, the hovering altitude and transmit power of UAVs were jointly optimized to reduce the cross-tier interference [22]. In [23], joint trajectory and transmit power optimization was investigated for UAV communication to maximize the average secrecy rate between UAV and ground UEs. Due to the signal enhancement and interference mitigation enabled by directional antennas, which are further affected by the 3D mobility of UAVs, the impact of transmit power management on UAV communication, particularly at different flight heights, needs to be newly investigated but has not been reported in the literature.

To address both challenges, in this paper, we propose a framework for modeling the downlink of UAV networks where, different from [9]–[11], [14]–[16], [18], UAVs are equipped with directional antennas. We assume that the ground UEs are associated with the serving UAV that provides the maximal receiving power while the UAVs in each tier employ the same transmit power for communication. The beam shaped by directional antenna has complicated impact

on the user association in UAV networks. For example, UEs may prefer a UAV located far away as serving ABS if the UAV is transmitting to the UEs in the main lobe. Moreover, for ground UEs located in the main lobe, directional antennas deployed at UAVs will improve the connectivity probability as they can easily activate their circuits, i.e., satisfying the receiving signal threshold. In contrast, for UEs located out of the main lobe, their connectivity probability reduces. Therefore, by employing directional antennas, there exists an interesting tradeoff between connectivity and coverage of UAV networks, whereas such tradeoff is unavailable for wireless networks employing omni-directional antennas. In this paper, we present a detailed analysis of the coverage and connectivity for the downlink of K-tier UAV networks. The stochastic geometry, which has been widely used for analyzing cellular networks [24], UAV networks [25], and millimeter-wave communication [26], is adopted in this paper to obtain closed-form results for performance evaluation. Our derivation results take into account the directivity of antenna elements, the receiving threshold, and the transmit output power. We note that, due to the impact of its antenna pattern, application of directional antenna leads to much more complicated performance analysis than in [9]–[11], [14]–[16], [18]. In [27], directional antennas with flat-top, sinc and cosine pattern functions are considered for millimeter-wave and cellular networks. However, the bounds for the achievable transmission rate are obtained by utilizing these approximate pattern functions, which fail to capture the directivity factor of directional antenna and its impact on the performance of wireless networks. In this paper, we adopt a novel tractable pattern function for directional antenna, which enables us to characterize the connectivity, association probability, and coverage probability of the considered UAV networks while capturing the impact of antenna directivity factor.

The contributions of this paper are as follows:

- We propose a tractable framework for modeling downlink transmission employing directional antennas in K-tier UAV networks. The associated probability distribution of communication distance between UEs and UAVs is analyzed taking into account the transmit output power, flying height, and directional antenna pattern of the UAVs. We find that a maximal transmission height of UAVs exists, independent of the directivity factor of directional antennas, within which UAVs can successfully connect the UEs.
- The probabilities of connecting the UAV network and associating with given tier of UAVs are both derived in closed form. We show that, with the adopting of directional antennas, ground UEs are prone to connect to UAVs flying at a large height.
- By investigating the coverage probability of downlink transmission in K-tier UAV networks, we show that UAV network equipped with directional antennas of large directivity factor can achieve much higher coverage probability than that with omni-directional antennas.

The remainder of this paper is organized as follows. In Section II, the system model of the considered multi-tier UAV networks employing directional antenna is presented. The probability distribution of communication distance for ground UEs served by the considered UAV networks is derived in Section III, where the impact of transmit output power, receiving threshold, and directivity of antenna element is revealed. In Section IV, the connectivity and the association probabilities of the considered UAV networks are analyzed, based on which the total coverage probability is further derived in Section V for LoS and NLoS transmissions. The derived results are validated via Monte Carlo simulation in Section VI, where the impact of maximal transmission distance, density and height of UAVs, and directivity factor of directional antenna on the downlink system performance is revealed. Finally, Section VII concludes the paper.

II. SYSTEM MODEL

A. NETWORK MODEL

As shown in Fig. 1, we consider downlink transmission in a 3D UAV network composing K tiers of ABSs. The ABSs in each tier are located at a given height but are randomly distributed horizontally. Let $(m_{i,k}, h_k)$ be the 3D location of ABS i in tier $k \in \{1, \cdots, K\}$, where h_k is the height and $m_{i,k}$ denotes the horizontal coordinate. We assume that the horizontal locations of ABSs in tier k, denoted by $\Phi_k = \{m_{i,k}; i = 1, 2, 3 \cdots\}$, follow a homogeneous Poisson Point Process (PPP) with density λ_k. The ABSs in tie k transmit signals with output power P_k. The UEs are randomly distributed on the ground with a height assumed to be zero. The locations of the UEs are modeled by a homogeneous PPP with density λ_u, denoted as $\Phi_u = \{x_i\}$, which is independent of Φ_k. For a tractable analysis, we assume that the ABSs of each tier move only horizontally while providing wireless communications in the considered multi-tier UAV networks. Since the speed of UAVs is relatively low, the locations of the ABSs in the air are considered to be fixed during the transmission of a data packet, whereas the ABSs may fly horizontally to different locations for the transmission of multiple data packets. Hence, the spatial distributions of the ABSs under random horizontal movements can still be captured by the PPP model. We assume that the channel fading keeps constant within a time slot, as commonly adopted for performance analysis of UAV networks [28], [29].

The ground UEs are associated with the ABSs in a tier that provide the strongest average receiving power. In this paper, we aim to analyze the performance of the considered multi-tier UAV networks and would ignore the terrestrial BSs which do not exist in the considered area or otherwise may employ orthogonal radio resources as the ABSs. Moreover, we focus on analyzing a typical UE U_0 located at the origin O and the typical cell C_0, where the ground UEs within C_0, including the typical UE, are served by the same UAV. The derivation results of the typical UE can be extended to other UEs on the ground by applying the Palm theory [30].

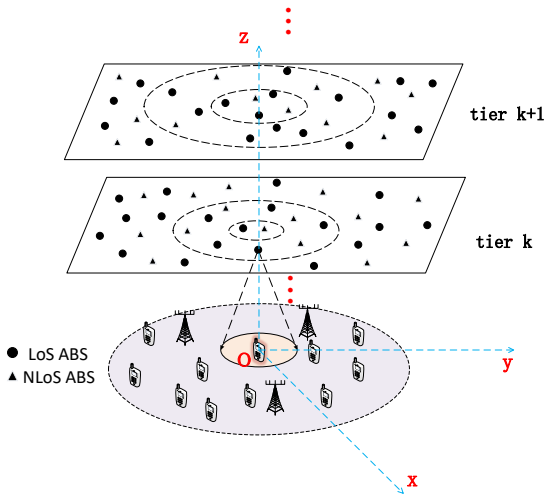

FIGURE 1. Illustration of the considered multi-tier UAV network model, where the ABSs serve the associated ground UEs within the coverage of their directional beams.

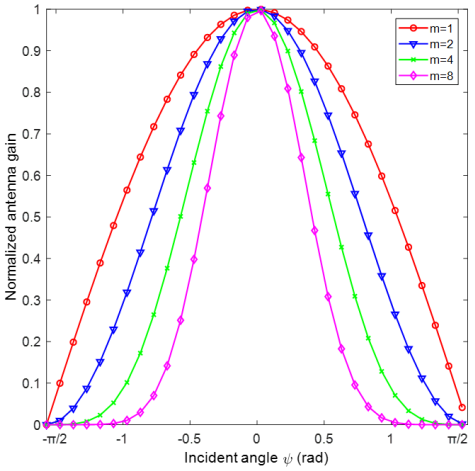

FIGURE 2. The normalized power pattern versus the incidence angle for different directivity factor m.

We assume open access within the UAV network, whereby the ground UEs are allowed to access ABSs in all tiers to maximize the coverage probability. However, all downlink transmission within the UAV network occupy the same spectrum, whereby the UAVs in networks can interfere with each other while serving the ground UEs.

B. DIRECTIONAL ANTENNA

The ABSs are equipped with directional antennas for communication with the ground UEs. In general, the antenna gain of a directional antenna, denoted as $G(\varphi, \psi)$, is a highly nonlinear function of the azimuth angle $\varphi \in [-\pi, \pi]$ and the incidence angle $\psi \in [0, \pi/2]$, which complicates the performance analysis. To simplify the derivations, in this paper, we consider conic directional antenna elements. The antenna gain of a conic antenna is given as $G(\varphi, \psi) = A_{er} \cos^m(\psi)$, where A_{er} is the maximal gain of antenna element and m is the directivity factor dependent on the beam shape [31].

The directivity D of antenna element is obtained from the following antenna equation [32]

$$D = \frac{4\pi}{\int_{-\pi}^{\pi} \int_{0}^{\frac{\pi}{2}} \left(G(\varphi, \psi)/A_{er}\right) \sin\psi d\psi d\varphi}. \tag{1}$$

By substituting $G(\varphi, \psi)$ into (1), the directivity of conic antenna is $D = 2(m + 1)$, which only depents on the directivity factor. The considered conic antenna gain model facilitates us to evaluate the impact of the shaped beam on the downlink performance of UAV networks. Fig. 2 shows the normalized power pattern $G(\varphi, \psi)/A_{er}$ for different m.

C. CHANNEL MODEL

The ABSs with a large elevation angle usually have a high likelihood of establishing LoS communication with the ground UEs [33]. As shown in Fig. 3, let θ be the elevation angle of the typical UAV in rad, which is the angle formed by the line from the UAV to the typical UE and the ground plane. In this paper, we assume that the ABSs always point the directional antennas toward the ground and, hence, we have $\theta = \pi/2 - \psi$. According to [33], the probability of establishing LoS communication from ABS at $m_{i,k}$ to the UE at O, denoted by $\boldsymbol{P}_L(\theta)$, is given as

$$\boldsymbol{P}_L(\theta) = \frac{1}{1 + ae^{-b(\theta - a)}}, \tag{2}$$

where a and b are constants capturing the statistical properties of the signal propagation environment. Consequently, the probability of NLoS communication is given by $\boldsymbol{P}_N(\theta) = 1 - \boldsymbol{P}_L(\theta)$.

Considering path loss and fading effect in the channel model, the receiving signal power at the typical UE is given as

$$P_{m_{i,k} \to o} \triangleq \begin{cases} P_k A_{er} \cos^m\left(\frac{\pi}{2} - \theta\right) G_k L_L^{-1}(m_{i,k}, o), \text{for LoS}, \\ P_k A_{er} \cos^m\left(\frac{\pi}{2} - \theta\right) H_k L_N^{-1}(m_{i,k}, o), \text{for NLoS}, \end{cases} \tag{3}$$

where P_k is the transmit power of the ABS located at $m_{i,k}$ and $A_{er} \cos^m\left(\frac{\pi}{2} - \theta\right)$ denotes the transmit antenna gain of the ABS with incidence angle $\psi = \frac{\pi}{2} - \theta$ (Note that the receiving antenna gain of ground UEs is assumed to be 1 in (3)). Moreover, $L(m_{i,k}, o) = \|m_{i,k}\|^{\alpha}$ models the path loss for signal propagation from $m_{i,k}$ to o, which is a function of the Euclidean distance between $m_{i,k}$ and o, $\|m_{i,k}\|$, and the path loss exponent α. We distinguish the path loss exponents for LoS and NLoS propagation by α_L and α_N, respectively, where $\alpha_L \leq \alpha_N$ usually holds. Moreover, the channel fading for LoS and NLoS propagation, denoted by G_k and H_k, are modeled as Nakagami-m_0 and Rayleigh random variables, respectively. Consequently, $G_k \sim \text{Gamma}(m_0)$ follows the Gamma distribution with scale parameter m_0 while $H_k \sim$

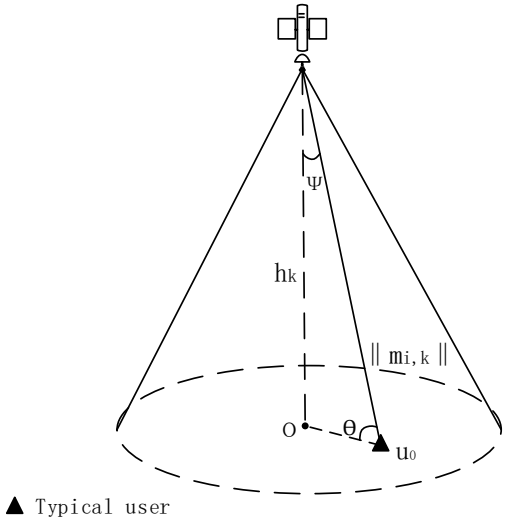

FIGURE 3. The footprint of a UAV with directional antenna.

$\exp(1)$ is exponentially distributed with unit mean power. For deriving the analytical results, the path loss exponent α_L and α_N are assumed to vary rarely across different tiers.

D. DOWNLINK SIGNAL TRANSMISSION

The ABSs should utilize large enough transmit output power to activate the receiver circuit at the UEs after combating the path loss and hence, the maximal allowable path loss between UAVs in tier k and the typical UE is given by $L_{\max,k} = P_k/\rho_c$, where ρ_c is the receiving signal threshold of the UEs. UAVs will fail to communicate with the UEs when their distances exceed $L_{\max,k}$. This implies that only a portion of UAVs can successfully connect the typical UE. Based on the PPP, the ABSs in tier k that can successfully connect the typical UE are uniformly distributed within a disc $b_k(o_k, r_k)$ centered at $o_k = (0, 0, h_k)$. The radius of the disc, r_k, can be derived based on the channel model (3), as will be revealed in Section III.

We note that the transmit power P_k and the receiving signal threshold ρ_c can jointly impact the performance of the considered multi-tier UAV networks. For example, the maximum distance between UAV and UEs, which impacts the connectivity of UAV networks, will be limited by the receiving signal threshold and the transmit power. Moreover, a higher transmit power P_k at UAVs will enable a large access region but leads to more interfering UAVs competing for the allocated spectrum. This reduces the signal-to-interference-plus-noise-ratio (SINR) and the coverage for UAV communication. Therefore, the joint impact of the transmit power and the receiving signal threshold on coverage and connectivity should be investigated in detail, which is the aim for the rest of this paper. The key notations used in this paper are listed in Table I.

TABLE 1. LIST OF KEY NOTATIONS

Symbols	Definitions
Φ_k, λ_k	PPP of kth tier ABSs and density
ρ_c	Receiving signal threshold of UEs
P_k	Transmit power of kth tier ABSs
α_L, α_N	Path loss exponent for LoS and NLoS channels
G	Nakagami-m_0 fading of LoS channel
H	Reighlay fading of NLoS channel
h_k	Height of kth tier ABSs
h^L_{max}, h^N_{max}	Maximal height of UAV transmission under LoS and NLoS communication
m^L_k, m^N_k	Maximal communication distance of UAVs in tier k under LoS and NLoS communications
$b_k(o_k, r_k)$	Disc with radius r_k and center o_k

III. COMMUNICATION DISTANCE DISTRIBUTION

In this section, we first derive the maximal distance within which the ABSs can successfully connect to the UEs. Then we characterize the probability distribution of the distance between the closest ABS in the k-th tier of the UAV networks and the ground UEs.

A. MAXIMAL COMMUNICATION DISTANCE

For the UAVs in tier k with height h_k, the maximum communication distances to the typical UE U_0 are calculated for LoS and NLoS propagation channels separately. When the ABS located at $m_{i,k}$ transmits in LoS channels, the receiving signal power at the typical UE is given as

$$P_r = P_k A_{er} \cos^m\left(\frac{\pi}{2} - \theta\right) G_k L_L^{-1}(m_{i,k}, o). \tag{4}$$

Since U_0 is located at the origin, thereafter we simply denote $L_L(x, o)$ and $L_N(x, o)$ as $L_L(x)$ and $L_N(x)$, respectively. In order to activate the receiver circuit, the average receiving power P_r should exceed the receiving threshold ρ_c, i.e.,

$$P_k A_{er} \left(\frac{h_k}{m_{i,k}}\right)^m \|m_{i,k}\|^{-\alpha_L} \geq \rho_c, \tag{5}$$

where $\cos(\pi/2 - \theta) = h_k/\|m_{i,k}\|$ according to Fig. 3.

Therefore, the maximal communication distance for the kth tier ABSs under LoS transmission is

$$m^L_k = \left(\frac{P_k A_{er} h_k^m}{\rho_c}\right)^{\frac{1}{\alpha_L + m}}. \tag{6}$$

Given the flying height of the ABSs in tier k, h_k, the radius of the disc of ABSs in tier k that can activate U_0 is further derived as

$$r^L_k = \sqrt{\left(\frac{P_k A_{er} h_k^m}{\rho_c}\right)^{\frac{2}{\alpha_L + m}} - h_k^2}. \tag{7}$$

Similarly, the maximal communication distance and radius for the kth tier ABSs under NLoS transmission are given as

$$m^N_k = \left(\frac{P_k A_{er} h_k^m}{\rho_c}\right)^{\frac{1}{\alpha_N + m}}$$
$$and\ r^N_k = \sqrt{\left(\frac{P_k A_{er} h_k^m}{\rho_c}\right)^{\frac{2}{\alpha_N + m}} - h_k^2}, \tag{8}$$

respectively. Since $\alpha_L \leq \alpha_N$, we have $r_k^L \geq r_k^N$. That is, the ABSs implementing LoS and NLoS communications to the UE may occupy different (though overlapping) regions. Therefore, the performance of LoS and NLoS communications should be evaluated separately.

We note that, constrained by the maximal transmit power of UAVs, $P_{\max}$, a maximal transmission height, $h_{\max}$, also exists for the ABSs. If the height of UAVs in tier k exceeds the maximal transmission height, i.e., $h_k > h_{\max}$, any UAV in this tier cannot successfully transmit signals to the typical UE. Based on (7) and (8), the maximal transmission height in tier k under LoS and NLoS communications can be obtained as

$$h_{\max}^L = \left(\frac{P_{\max}A_{er}}{\rho_c}\right)^{1/\alpha_L} \text{ and } \quad h_{\max}^N = \left(\frac{P_{\max}A_{er}}{\rho_c}\right)^{1/\alpha_N}. \tag{9}$$

Note that the maximal transmission height is independent of the directivity factor of directional antenna, m. This is because the maximal transmission height appears when the ABS is located at the center of disc b_k. In this case, the elevation angle is $\theta = \pi/2$ and the maximal antenna gain A_{er} is achieved independent of the directivity factor m.

B. DISTRIBUTION OF COMMUNICATION DISTANCE

Recall that, in tier k, only the ABSs located within disc b_k can successfully communicate with the typical UE. The communication distance between the ABSs and the UE under LoS and NLoS communication, denoted by random variables D_k^L and D_k^N, have the following probability density functions (PDFs)

$$f_{D_k^L}(d_k) = \begin{cases} \frac{2d_k}{(r_k^L)^2}, & \text{if } h_k \leq d_k \leq m_k^L, \\ 0, \text{ otherwise}, \end{cases} \tag{10}$$

and

$$f_{D_k^N}(d_k) = \begin{cases} \frac{2d_k}{(r_k^N)^2}, & \text{if } h_k \leq d_k \leq m_k^N, \\ 0, \text{ otherwise}, \end{cases} \tag{11}$$

where r_k^L, r_k^N, m_k^L, and m_k^N are given in (6)–(8). Note that (10) and (11) can be obtained similar to Lemmas 1 and 2 in [28], which conclude that a given number of UAV nodes uniformly distributed within a finite region follow a binomial point process (BPP).

Lemma 1: Based on the maximal transmission distance and the uniform location distribution of UAVs in tier k, the average number of ABSs implementing LoS and NLoS communications are given as

$$\mathbb{E}\left[n_k^L\right] = 2\pi\lambda_k \int_0^{r_k^L} \frac{x}{1 + ae^{-b\left(\arctan\left(\frac{h_k}{x}\right) - a\right)}} dx, \tag{12}$$

and

$$\mathbb{E}\left[n_k^N\right] = 2\pi\lambda_k \int_0^{r_k^N} \frac{xae^{-b\left(\arctan\left(\frac{h_k}{x}\right) - a\right)}}{1 + ae^{-b\left(\arctan\left(\frac{h_k}{x}\right) - a\right)}} dx. \tag{13}$$

Proof: Recall that the UAV with elevation angle θ can implement LoS communication with probability given in (2). The elevation angle can be expressed as $\theta = \arctan\left(\frac{h_k}{d}\right)$, where d is the distance between UAV in tier k and o_k. The number of UAVs in tier k implementing LoS communication is then given by

$$\begin{aligned}\mathbb{E}\left[n_k^L\right] &= \int_0^{2\pi}\int_0^{r_k^L} \lambda_k \frac{x}{1 + ae^{-b\left(\arctan\left(\frac{h_k}{x}\right) - a\right)}} dx d\phi_k \\ &= 2\pi\lambda_k \int_0^{r_k^L} \frac{x}{1 + ae^{-b\left(\arctan\left(\frac{h_k}{x}\right) - a\right)}} dx, \end{aligned} \tag{14}$$

where ϕ_k is the angle subtended by line from the ABS to o_k and the x-axis in disc b_k, and is uniformly distributed within $[0, 2\pi]$. The UAVs failing to implement LoS communication will communicate under NLoS condition. The number of UAVs in tier k implementing NLoS communication is

$$\begin{aligned}\mathbb{E}\left[n_k^N\right] &= \int_0^{2\pi}\int_0^{r_k^N} \lambda_k x \left(1 - \frac{1}{1 + ae^{-b\left(\arctan\left(\frac{h_k}{x}\right) - a\right)}}\right) dx d\phi_k \\ &= 2\pi\lambda_k \int_0^{r_k^N} \frac{xae^{-b\left(\arctan\left(\frac{h_k}{x}\right) - a\right)}}{1 + ae^{-b\left(\arctan\left(\frac{h_k}{x}\right) - a\right)}} dx, \end{aligned} \tag{15}$$

which complete the proof. ■

The typical UE is associated with the ABS providing the maximal average receiving power. As all UAVs in tier k employ the same transmit power P_k, the ABS in tier k having the closest distance will provide maximal average receiving power for the typical UE. This motivates us to derive the probability distribution of the closest distance between ABSs in tier k and the typical UE and the result is included in the following lemma.

Lemma 2: The PDF of the closest distance between the ABS in tier k and the typical UE under LoS transmission is

$$f_{X_k^L}(x) = \begin{cases} \mathbb{E}\left[n_k^L\right]\left(1 - \frac{x^2 - (h_k)^2}{(r_k^L)^2}\right)^{\mathbb{E}\left[n_k^L\right]-1} \cdot \frac{2x}{(r_k^L)^2}, \text{if } h_k \leq x \leq m_k^L, \\ 0, \text{ otherwise}, \end{cases} \tag{16}$$

where $\mathbb{E}\left[n_k^L\right]$ is the average number of UAVs in tier k implementing LoS communication as given in (14).

Proof: For the ABSs in tier k having the closest distance, the cumulative distribution function (CDF) of the closest distance to the typical UE is obtained as

$$\begin{aligned} F_{X_k^L}(x) &= 1 - \mathbb{P}\left(X_k^L > x\right) \\ &= 1 - \mathbb{P}\left(\min\left\{X_{k,1}^L, X_{k,2}^L, \ldots, X_{k,n_k^L}^L\right\} > x\right) \\ &= 1 - \left[1 - F_{X_k^L}(x)\right]^{\mathbb{E}\left[n_k^L\right]}. \end{aligned} \tag{17}$$

The PDF can obtain from the derivation of (17) as

$$\begin{aligned} f_{X_k^L}(x) &= \frac{dF_{X_k^L}(x)}{dx} \\ &= \mathbb{E}\left[n_k^L\right]\left[1 - F_{X_k^L}(x)\right]^{\mathbb{E}\left[n_k^L\right]-1} f_{X_k^L}(x) \\ &= \mathbb{E}\left[n_k^L\right]\left(1 - \frac{x^2 - (h_k)^2}{(r_k^L)^2}\right)^{\mathbb{E}\left[n_k^L\right]-1} \cdot \frac{2x}{(r_k^L)^2}. \end{aligned} \tag{18}$$

■

Similarly, the PDF of the closest distance between the ABSs in tier k and the typical UE under NLoS transmission can be obtained as

$$f_{X_k^N}(x)=\begin{cases}\mathbb{E}\left[n_k^N\right]\left(1-\frac{x^2-(h_k)^2}{\left(r_k^N\right)^2}\right)^{\mathbb{E}\left[n_k^N\right]-1}\cdot\frac{2x}{\left(r_k^N\right)^2}, & \text{if } h_k\le x\le m_k^N,\\ 0, \text{ otherwise.}\end{cases} \tag{19}$$

IV. CONNECTIVITY AND ASSOCIATION PROBABILITIES OF UAV NETWORKS

In the considered UAV networks, the ground UE can connect with an ABS provided its receiver circuit can be activated by the ABS. Meanwhile, according to the association policy, the ground UE will associate with the ABSs in any tier that provide the maximum average receiving power. In this section, we will analyze the connection and association probabilities for the considered multi-tier UAV networks.

A. CONNECTIVITY PROBABILITY OF UAV NETWORKS

Based on the analysis in Section III, the typical UE can connect to the considered UAV networks if and only if there exists $k\in\{1,\cdots,K\}$ such that at least an ABS in tier k is located within disc b_k. On the contrary, for ABSs spatially distributed according to a PPP, the probability that ABSs in tier k cannot connect with the typical UE, which is given by $\mathbb{P}\left\{\Phi_i\cap b_i=\phi,\forall i=1,\cdots,K\right\}$, can be characterized in Lemma 3.

Lemma 3: The probability that the typical UE cannot connect with UAV networks is

$$\mathbb{P}\left\{\Phi_i\cap b_i=\phi,\forall i=1,\cdots,K\right\}= \exp\left(-\pi\sum_{k=1}^{K}\lambda_k\left(\left(\frac{P_kA_{er}h_k^m}{m_0\rho_c}\right)^{\frac{2}{m+\alpha_L}}\frac{\Gamma\left(\frac{2}{\alpha_L+m}+m_0\right)}{\Gamma\left(m_0\right)}-h_k^2\right)\right). \tag{20}$$

Proof: The typical UE cannot connect with the ABSs in tier k if and only if it can neither connect with the ABSs implementing LoS nor NLoS communication, i.e.,

$$\mathbb{P}\{\Phi_k\cap b_k=\phi\}=\mathbb{P}\{\Phi_k\cap b_{k,L}=\phi \text{ and } \Phi_k\cap b_{k,N}=\phi\}. \tag{21}$$

Since $b_{k,L}$ and $b_{k,N}$ have the same center o_k, $b_{k,L}$ and $b_{k,N}$ would overlap with each other. Moreover, as $r_k^N\le r_k^L$, $b_{k,L}$ covers $b_{k,N}$ and hence, $\mathbb{P}\left\{\Phi_k\cap b_k=\phi\right\}=\mathbb{P}\left\{\Phi_k\cap b_{k,L}=\phi\right\}$. Consequently, the typical UE cannot connect with the ABSs if all ABSs in tier k are located outside the circle $b_{k,L}$. Thus, the probability that the typical UE cannot connect with the ABSs implementing LoS communication in tier k is

$$\begin{aligned}&\mathbb{P}\left\{\Phi_k\cap b_k=\phi\right\}\\ &=\mathbb{P}\left(\max_{m_{i,k}\in\Phi_k}P_kA_{er}\cos^m\left(\frac{\pi}{2}-\theta\right)G_kL_L^{-1}\left(m_{i,k},o\right)<\rho_c\right)\\ &=\mathbb{P}\left(P_kA_{er}\frac{h_k^m}{\left(r^2+h_k^2\right)^{m/2}}G_k\left(r^2+h_k^2\right)^{-\alpha_L/2}<\rho_c\right)\\ &=\mathbb{P}\left(r^2>\left(\frac{P_kA_{er}G_kh_k^m}{\rho_c}\right)^{\frac{2}{m+\alpha_L}}-h_k^2\right)\\ &=\exp\left(-\pi\lambda_k\left(\left(\frac{P_kA_{er}h_k^m}{\rho_c}\right)^{\frac{2}{m+\alpha_L}}\mathbb{E}\left[G_k^{\frac{2}{m+\alpha_L}}\right]-h_k^2\right)\right)\\ &=\exp\left(-\pi\lambda_k\left(\left(\frac{P_kA_{er}h_k^m}{m_0\rho_c}\right)^{\frac{2}{m+\alpha_L}}\frac{\Gamma\left(\frac{2}{\alpha_L+m}+m_0\right)}{\Gamma\left(m_0\right)}-h_k^2\right)\right).\end{aligned} \tag{22}$$

As the point processes of ABSs in different tiers are independent of each other, we have

$$\begin{aligned}&\mathbb{P}\left\{\Phi_i\cap b_i=\phi,\forall i=1,\cdots,K\right\}\\ &=\prod_{k=1}^{K}\mathbb{P}\left\{\Phi_k\cap b_k=\phi\right\}\\ &=\exp\left(-\pi\sum_{k=1}^{K}\lambda_k\left(\left(\frac{P_kA_{er}h_k^m}{m_0\rho_c}\right)^{\frac{2}{m+\alpha_L}}\frac{\Gamma\left(\frac{2}{\alpha_L+m}+m_0\right)}{\Gamma\left(m_0\right)}-h_k^2\right)\right),\end{aligned} \tag{23}$$

which complete the proof. ■

Based on Lemma 3, the probability that the typical UE can connect with the K-tier UAV networks is

$$1-\exp\left(-\pi\sum_{k=1}^{K}\lambda_k\left(\left(\frac{P_kA_{er}h_k^m}{m_0\rho_c}\right)^{\frac{2}{m+\alpha_L}}\frac{\Gamma\left(\frac{2}{\alpha_L+m}+m_0\right)}{\Gamma\left(m_0\right)}-h_k^2\right)\right). \tag{24}$$

From (24) we observe that the directivity of directional antenna, m, highly impacts the connection probability of the ground UEs. It can be further proved that the probability of UE connecting UAV networks decreases with m. This is because, by utilizing directional antennas, the radius r_k of b_k will decrease with m and more UAVs are located out of b_k. Therefore, by employing directional antennas, the region where UAVs can successfully connect with the UE will reduce and less ground UEs can communicate with the UAV networks.

B. ASSOCIATION PROBABILITY OF UAV NETWORKS

When the typical UE can connect with the UAV networks, it will associate with the serving ABS providing the maximal average receiving power. The probability that the typical UE is associated with the ABS in tier k under LoS communication, denoted as $\mathbb{P}\left(\mathrm{A}^L=k\right)$, is given in the following theorem.

Theorem 1: Under LoS communication, the typical UE will be associated to the ABSs in tier k with a probability given as

$$\begin{aligned}&\mathbb{P}\left(\mathrm{A}^L=k\right)\\&=\int_{h_k}^{m_k^L}\prod_{j=1,j\neq k}^{K}\left(1-\frac{\left(\frac{P_j}{P_k}\right)^{\frac{2}{m+\alpha_L}}\left(\frac{h_j}{h_k}\right)^{\frac{2m}{m+\alpha_L}}r^2-h_j^2}{\left(r_j^L\right)^2}\right)^{\mathbb{E}\left[n_j^L\right]}\\&\cdot\prod_{j=1}^{K}\left(1-\frac{\left(\frac{P_j}{P_k}\right)^{\frac{2}{m+\alpha_N}}\left(\frac{h_j}{h_k}\right)^{\frac{2m}{m+\alpha_N}}r^{\frac{2(m+\alpha_L)}{m+\alpha_N}}-h_j^2}{\left(r_j^N\right)^2}\right)^{\mathbb{E}\left[n_j^N\right]}\\&\cdot\mathbb{E}\left[n_k^L\right]\left(1-\frac{r^2-(h_k)^2}{\left(r_k^L\right)^2}\right)^{\mathbb{E}\left[n_k^L\right]-1}\cdot\frac{2r}{\left(r_k^L\right)^2}dr.\end{aligned}\tag{25}$$

Proof: As the UAVs can implement both LoS and NLoS communications, the associated ABS in tier k for serving the typical UE has to satisfy two independent conditions. For association with the ABSs under LoS transmission, the serving ABS has to provide the maximal average receiving power among all ABSs. Meanwhile, the receiving power from the serving ABS has to exceed that from all ABSs under NLoS transmissions. Let R be the closest distance between the UAVs in tier k and the typical UE. We have

$$\begin{aligned}&\mathbb{P}\left(\mathrm{A}^L=k\right)=\\&\mathbb{E}_R\left[\mathbb{P}_L\left(P_{r,k}^L(R)>\max_{j,j\neq k}P_{r,j}^L\right)\cdot\mathbb{P}_L\left(P_{r,k}^L(R)>\max_{j=1,\cdots,K}P_{r,j}^N\right)\right].\end{aligned}\tag{26}$$

As the ABSs implement LoS and NLoS communications independently, we can calculate (26) as

$$\begin{aligned}&\mathbb{P}\left(\mathrm{A}^L=k\right)\\&=\mathbb{E}_R\left[\prod_{j=1,j\neq k}^{K}\mathbb{P}_L\left(P_{r,k}^L(R)>P_{r,j}^L\right)\cdot\prod_{j=1}^{K}\mathbb{P}_L\left(P_{r,k}^L(R)>P_{r,j}^N\right)\right]\\&=\mathbb{E}_R\left[\prod_{j=1j\neq k}^{K}\mathbb{P}_L\left(P_kA_{er}\left(\frac{h_k}{R}\right)^m G_kR^{-\alpha_L}>P_jA_{er}\left(\frac{h_j}{R_j}\right)^m G_kR_j^{-\alpha_L}\right)\right.\\&\left.\cdot\prod_{j=1}^{K}\mathbb{P}_L\left(P_kA_{er}\left(\frac{h_k}{R}\right)^m G_kR^{-\alpha_L}>P_jA_{er}\left(\frac{h_j}{R_j}\right)^m H_kR_j^{-\alpha_N}\right)\right]\\&=\int_{h_k}^{m_k^L}\prod_{j=1,j\neq k}^{K}\mathbb{P}_L\left(R_j>\left(\frac{P_j}{P_k}\right)^{\frac{1}{m+\alpha_L}}\left(\frac{h_j}{h_k}\right)^{\frac{m}{m+\alpha_L}}r\right)\\&\cdot\prod_{j=1}^{K}\mathbb{P}_L\left(R_j>\left(\frac{P_j}{P_k}\right)^{\frac{1}{m+\alpha_N}}\left(\frac{h_j}{h_k}\right)^{\frac{m}{m+\alpha_N}}r^{\frac{m+\alpha_L}{m+\alpha_N}}\right)f_R(r)dr\\&=\int_{h_k}^{m_k^L}\prod_{j=1,j\neq k}^{K}\left(1-\frac{\left(\frac{P_j}{P_k}\right)^{\frac{2}{m+\alpha_L}}\left(\frac{h_j}{h_k}\right)^{\frac{2m}{m+\alpha_L}}r^2-h_j^2}{\left(r_j^L\right)^2}\right)^{\mathbb{E}\left[n_j^L\right]}\\&\cdot\prod_{j=1}^{K}\left(1-\frac{\left(\frac{P_j}{P_k}\right)^{\frac{2}{m+\alpha_N}}\left(\frac{h_j}{h_k}\right)^{\frac{2m}{m+\alpha_N}}r^{\frac{2(m+\alpha_L)}{m+\alpha_N}}-h_j^2}{\left(r_j^N\right)^2}\right)^{\mathbb{E}\left[n_j^N\right]}f_R(r)dr,\end{aligned}\tag{27}$$

where $f_R(r)$ has been obtained in (16). Theorem 1 can be proved by Substituting (16) into (27). ■

Under NLoS transmission, the probability of association to the ABS in tier k can be similarly obtained as

$$\begin{aligned}&\mathbb{P}\left(\mathrm{A}^N=k\right)\\&=\int_{h_k}^{m_k^N}\prod_{j=1,j\neq k}^{K}\left(1-\frac{\left(\frac{P_j}{P_k}\right)^{\frac{2}{m+\alpha_N}}\left(\frac{h_j}{h_k}\right)^{\frac{2m}{m+\alpha_N}}r^2-h_j^2}{\left(r_j^N\right)^2}\right)^{\mathbb{E}\left[n_j^N\right]}\\&\cdot\prod_{j=1}^{K}\left(1-\frac{\left(\frac{P_j}{P_k}\right)^{\frac{2}{m+\alpha_L}}\left(\frac{h_j}{h_k}\right)^{\frac{2m}{m+\alpha_L}}r^{\frac{2(m+\alpha_N)}{m+\alpha_L}}-h_j^2}{\left(r_j^L\right)^2}\right)^{\mathbb{E}\left[n_j^L\right]}\\&\cdot\mathbb{E}\left[n_k^N\right]\left(1-\frac{r^2-(h_k)^2}{\left(r_k^N\right)^2}\right)^{\mathbb{E}\left[n_k^N\right]-1}\frac{2r}{\left(r_k^N\right)^2}dr.\end{aligned}\tag{28}$$

Let X_k be the distance between the typical UE and its serving ABS when the typical UE is associated with the ABS in tier k. Recall that the ABSs which can connect to the typical UE must be located within disc b_k. Given the location distribution of ABSs in tier k, cf. Lemma 2, the PDF of X_k can be derived in the following theorem.

Theorem 2: Under LoS transmission, the PDF of X_k, the distance between the typical UE and its serving ABS in tier k, is given as

$$\begin{aligned}&f_{X_k}(x)=\\&\frac{1}{\mathbb{P}(\mathrm{A}^L=k)}\prod_{j=1,j\neq k}^{K}\left(\left[1-\frac{\left(\frac{P_j}{P_k}\right)^{\frac{2}{m+\alpha_L}}\left(\frac{h_j}{h_k}\right)^{\frac{2m}{m+\alpha_L}}x^2-h_j^2}{\left(r_j^L\right)^2}\right]^{\mathbb{E}\left[n_j^L\right]}\right)\\&\cdot\prod_{j=1}^{K}\left(\left[1-\frac{\left(\frac{P_j}{P_k}\right)^{\frac{2}{m+\alpha_N}}\left(\frac{h_j}{h_k}\right)^{\frac{2m}{m+\alpha_N}}x^{\frac{2(m+\alpha_L)}{m+\alpha_N}}-h_j^2}{\left(r_j^N\right)^2}\right]^{\mathbb{E}\left[n_j^N\right]}\right)\\&\cdot\mathbb{E}\left[n_k^L\right]\left(1-\frac{x^2-(h_k)^2}{\left(r_k^L\right)^2}\right)^{\mathbb{E}\left[n_k^L\right]-1}\cdot\frac{2x}{\left(r_k^L\right)^2}.\end{aligned}\tag{29}$$

Proof: Let R_k be the distance between the typical UE and its serving ABS. Under the condition that the associated ABS is located in tier k and has LoS communication with the UE, we have

$$\mathbb{P}\left\{R_k^L>x|A_k^L\right\}=\frac{\mathbb{P}\left\{R_k^L>x,\mathrm{A}^L=k\right\}}{\mathbb{P}\left(\mathrm{A}^L=k\right)},\tag{30}$$

with

$$\begin{aligned}
&\mathbb{P}\left\{R_k^L > x, \mathrm{A}^L = k\right\} \\
=&\mathbb{P}_L\left(R_k^L > x, P_{r,k}^L\left(R_k\right) > \max_{j,j\neq k} P_{r,j}^L \text{ and } P_{r,k}^L\left(R_k\right) > \max_{j=1,\cdots,K} P_{r,j}^N\right) \\
=&\int_x^{m_k^L} \prod_{j=1,j\neq k}^{K} \mathbb{P}_L\left(R_j > \left(\frac{P_j}{P_k}\right)^{\frac{1}{m+\alpha_L}} \left(\frac{h_j}{h_k}\right)^{\frac{m}{m+\alpha_L}} r\right) \\
&\cdot \prod_{j=1}^{K} \mathbb{P}_L\left(R_j > \left(\frac{P_j}{P_k}\right)^{\frac{1}{m+\alpha_N}} \left(\frac{h_j}{h_k}\right)^{\frac{m}{m+\alpha_N}} r^{\frac{m+\alpha_L}{m+\alpha_N}}\right) f_{R_k}(r)dr \\
=&\int_x^{m_k^L} \prod_{j=1 j\neq k}^{K} \left(1 - \frac{\left(\frac{P_j}{P_k}\right)^{\frac{2}{m+\alpha_L}} \left(\frac{h_j}{h_k}\right)^{\frac{2m}{m+\alpha_L}} r^2 - h_j^2}{\left(r_j^L\right)^2}\right)^{\mathbb{E}\left[n_j^N\right]} \\
&\cdot \prod_{j=1}^{K} \left(1 - \frac{\left(\frac{P_j}{P_k}\right)^{\frac{2}{m+\alpha_N}} \left(\frac{h_j}{h_k}\right)^{\frac{2m}{m+\alpha_N}} r^{\frac{2(m+\alpha_L)}{m+\alpha_N}} - h_j^2}{\left(r_j^N\right)^2}\right)^{\mathbb{E}\left[n_j^L\right]} f_{R_k}(r)dr.
\end{aligned} \tag{31}$$

Moreover, substituting (25) into (30), we have

$$\begin{aligned}
&\mathbb{P}\left\{X_k > x\right\} = \\
&\frac{1}{\mathbb{P}\left(\mathrm{A}^L = k\right)} \int_x^{m_k^L} \prod_{j=1 j\neq k}^{K} \left(1 - \frac{\left(\frac{P_j}{P_k}\right)^{\frac{2}{m+\alpha_L}} \left(\frac{h_j}{h_k}\right)^{\frac{2m}{m+\alpha_L}} r^2 - h_j^2}{\left(r_j^L\right)^2}\right)^{\mathbb{E}\left[n_j^L\right]} \\
&\cdot \prod_{j=1}^{K} \left(1 - \frac{\left(\frac{P_j}{P_k}\right)^{\frac{2}{m+\alpha_N}} \left(\frac{h_j}{h_k}\right)^{\frac{2m}{m+\alpha_N}} r^{\frac{2(m+\alpha_L)}{m+\alpha_N}} - h_j^2}{\left(r_j^N\right)^2}\right)^{\mathbb{E}\left[n_j^N\right]} f_{R_k}(r)dr.
\end{aligned} \tag{32}$$

Finally, Theorem 2 can be proved be taking $f_{X_k}(x) = \frac{d(1-\mathbb{P}\{X_k>x\})}{dx}$. ■

Meanwhile, under the condition that the serving ABS with LoS transmission is in tier k and has distance R_k to the UE, other ABSs in the UAV networks will interfere the desired signals due to the full spectrum reuse among the ABSs. The receiving interference power at the typical UE caused from other interfering ABSs should be less than the receiving power from the serving ABS. Define $X_{I,j}$ as the distance between the typical UE and an interfering ABS in tier j. The PDF of $X_{I,j}$ can be described in the following lemma..

Lemma 4: Given that the serving ABS is located in tier k at a distance of R_k, the PDF of the distance between the typical UE and interfering ABS in tier j, $X_{I,j}$, with LoS transmission is

$$f\left(x_{I,j} > R_k\right) = \begin{cases} \frac{2x_{I,j}}{m_j^2 - \left(\frac{P_j}{P_k}\right)^{\frac{2}{m+\alpha_L}} \left(\frac{h_j}{h_k}\right)^{\frac{2m}{m+\alpha_L}} R_k^2} \\ \cdot \left(\frac{P_j}{P_k}\right)^{\frac{1}{m+\alpha_L}} \left(\frac{h_j}{h_k}\right)^{\frac{m}{m+\alpha_L}}, \text{ if } R_k < m_j, \\ 0, \text{otherwise.} \end{cases} \tag{33}$$

Proof: As the distance between the typical UE and the serving ABS in tier k is R_k, the distance from the interfering ABS in tier j to the UE should satisfy

$$P_k A_{er} \left(h_k/R\right)^m \left(R_k\right)^{-\alpha_L} > P_j A_{er} \left(\frac{h_j}{X_{I,j}}\right)^m \left(X_{I,j}\right)^{-\alpha_L}. \tag{34}$$

We obtain that $X_{I,j} > \left(\frac{P_j}{P_k}\right)^{\frac{1}{m+\alpha_L}} \left(\frac{h_j}{h_k}\right)^{\frac{m}{m+\alpha_L}} R_k$. Hence,

$$f\left(x_{I,j} > R_k\right) = \frac{2x_{I,j}}{m_j^2 - \left(\frac{P_j}{P_k}\right)^{\frac{2}{m+\alpha_N}} \left(\frac{h_j}{h_k}\right)^{\frac{2m}{m+\alpha_L}} {R_k}^2}, \tag{35}$$

which completes the proof. ■

Similarly, the PDF for the distance between the typical UE and an interfering ABS in tier j, $X_{I,j}$, with NLoS transmission is

$$f(x_{I,j} > R_k) = \begin{cases} \frac{2x_{I,j}}{m_j^2 - \left(\frac{P_j}{P_k}\right)^{\frac{2}{m+\alpha_N}} \left(\frac{h_j}{h_k}\right)^{\frac{2m}{m+\alpha_N}} R_k^{\frac{2(m+\alpha_L)}{m+\alpha_N}}} \\ \cdot \left(\frac{P_j}{P_k}\right)^{\frac{1}{m+\alpha_N}} \left(\frac{h_j}{h_k}\right)^{\frac{m}{m+\alpha_N}}, \text{ if } R_k^{\frac{m+\alpha_L}{m+\alpha_N}} < m_j, \\ 0, \text{ otherwise.} \end{cases} \tag{36}$$

V. ANALYSIS OF COVERAGE PROBABILITY

Based on the association probability in Section IV, we can further derive the coverage probability of the K-tier UAV networks. For this purpose, we first have to derive the Laplace transform of the aggregated interference power caused from the interfering ABSs.

Based on the distance distribution of the serving ABS and interfering ABSs, the total coverage probability of the K-tier UAV networks, P_c, can be calculated as

$$P_c = \sum_{k=1}^{n} \left(\mathbb{P}^L(A=k)A_k^L + \mathbb{P}^N(A=k)A_k^N\right), \tag{37}$$

where $\mathbb{P}^L(A=k)$ ($\mathbb{P}^N(A=k)$) is the coverage probability conditioning on that the serving ABS is in tier k and has LoS (NLoS) transmission. A_k^L and A_k^N are the association probabilities that the serving ABS in tier k has LoS and NLoS transmissions, respectively.

Given that the distance from the serving ABS in tier k with LoS or NLoS transmission is $R_{k,o}$, the signal-to-interference ratio (SIR) at the typical UE can be given as

$$\begin{aligned}
\mathrm{SIR}_k^L\left(R_{k,o}\right) &= \frac{P_k A_{er} \left(\frac{h_k}{R_{k,o}}\right)^m G_{r_{k,o}} R_{k,o}^{-\alpha_L}}{I_L + I_N}, \\
\mathrm{SIR}_k^N\left(R_{k,o}\right) &= \frac{P_k A_{er} \left(\frac{h_k}{R_{k,o}}\right)^m H_{r_{k,o}} R_{k,o}^{-\alpha_N}}{I_L + I_N},
\end{aligned} \tag{38}$$

where I_L and I_N are aggregated interference powers from interfering ABSs under LoS and NLoS transmissions, respectively.

Based on [34], the coverage probability $\mathbb{P}^L(A=k)$ can be defined as

$$\mathbb{P}^L(A=k) = \mathbb{E}_{R_{k,o}}\left[\mathbb{P}\left\{\mathrm{SIR}_k^L\left(R_{k,o}\right) \leq \mathrm{T}\right\}\right], \tag{39}$$

where T is the SIR threshold for downlink transmission. Moreover, given that the distance of the serving ABS is R, the Laplace transform of interference power with LoS transmission, I_L, is given in the following Lemma.

Lemma 5: Given that the serving ABS with LoS transmission is located at a distance of R away from the typical UE, the Laplace transform of the interference power, I_L, is given as

$$\mathcal{L}_I^L(s|R) = \mathbb{E}_{I_L}^L\left[\exp\left(-sI_L\right)|R\right] \mathbb{E}_{I_N}^L\left[\exp\left(-sI_N\right)|R\right], \tag{40}$$

where

$$\mathbb{E}_{I_L}^{L}\left[\exp\left(-sI_L\right)|R\right] = \prod_{j=1,j\neq k}^{K}\int_{\left(\frac{P_j}{P_k}\right)^{\frac{1}{m+\alpha_L}}\left(\frac{h_j}{h_k}\right)^{\frac{m}{m+\alpha_L}}R}^{m_j}\left(1+\frac{sP_jA_{er}h_j^m x^{-(\alpha_L+m)}}{m_0}\right)^{-m_0\mathbb{E}\left[n_j^L\right]} \cdot \frac{2x}{m_j^2-R^2\left(\frac{P_j}{P_k}\right)^{\frac{2}{m+\alpha_L}}\left(\frac{h_j}{h_k}\right)^{\frac{2m}{m+\alpha_L}}}dx \cdot \int_{R}^{m_k}\left(1+\frac{sP_kA_{er}h_j^m x^{-(\alpha_L+m)}}{m_0}\right)^{-m_0\left(\mathbb{E}\left[n_k^L\right]-1\right)}\frac{2x}{m_k^2-R^2}dx, \tag{41}$$

and

$$\mathbb{E}_{I_N}^{L}\left[\exp\left(-sI_N\right)|R\right] = \prod_{j=1}^{K}\int_{\left(\frac{P_j}{P_k}\right)^{\frac{1}{m+\alpha_N}}\left(\frac{h_j}{h_k}\right)^{\frac{m}{m+\alpha_N}}R}^{m_j}\left(\frac{1}{1+sP_jA_{er}h_j^m x^{-(\alpha_N+m)}}\right)^{\mathbb{E}\left[n_j^N\right]} \cdot \frac{2x}{m_j^2-\left(\frac{P_j}{P_k}\right)^{\frac{2}{m+\alpha_N}}\left(h_j/h_k\right)^{\frac{2m}{m+\alpha_N}}R^{\frac{2(m+\alpha_L)}{m+\alpha_N}}}dx. \tag{42}$$

Proof: The Laplace transform of the interference power, $I_L + I_N$, can be derived as

$$\begin{aligned}\mathcal{L}_I^L(s|R) &= \mathbb{E}_I^L\left[\exp\left(-s\left(I_L+I_N\right)\right)|R\right] \\ &= \mathbb{E}_{I_L}^L\left[\exp\left(-sI_L\right)|R\right]\mathbb{E}_{I_N}^L\left[\exp\left(-sI_N\right)|R\right].\end{aligned} \tag{43}$$

Herein, the Laplace transform of the interference power caused by ABSs with LoS transmission is given in (44). Moreover, the interference power caused from ABSs with NLoS transmission has the following Laplace transform,

$$\begin{aligned}&\mathbb{E}_{I_N}\left[\exp\left(-sI_N\right)|R\right] \\ &= \mathbb{E}_{I_L}\left[\exp\left(-s\sum_{j=1}^{K}\sum_{i=1}^{E\left[n_j^N\right]}I_{i,j}\right)|R\right] \\ &= \mathbb{E}_{I_L}\left[\prod_{j=1}^{K}\prod_{i=1}^{E\left[n_j^N\right]}\exp\left(-sP_jA_{er}\left(\frac{h_j}{u_{i,j}}\right)^m H_{u_{i,j}}u_{i,j}^{-\alpha_N}\right)|R\right] \\ &= \prod_{j=1}^{K}\mathbb{E}_{U_{N,j}^L,H_j^L}\left[\prod_{i=1}^{E\left[n_j^N\right]}\exp\left(-SP_jA_{er}h_j^m H_{u_{i,j}}u_{i,j}^{-(\alpha_N+m)}\right)|R\right] \\ &= \prod_{j=1}^{K}\mathbb{E}_{U_{N,j}^L}\left[\prod_{i=1}^{E\left[n_j^N\right]}\mathbb{E}_H\left[\exp\left(-sP_jA_{er}h_j^m Hu_{i,j}^{-(\alpha_N+m)}\right)\right]|R\right] \\ &= \prod_{j=1}^{K}\mathbb{E}_{U_{N,j}^L}\left[\left[\frac{1}{1+sP_jA_{er}h_j^m u_{i,j}^{-(\alpha_N+m)}}|R\right]^{E\left[n_j^N\right]}\right] \\ &= \prod_{j=1}^{K}\int_{\left(\frac{P_j}{P_k}\right)^{\frac{1}{m+\alpha_N}}\left(\frac{h_j}{h_k}\right)^{\frac{m}{m+\alpha_N}}R^{\frac{m+\alpha_L}{m+\alpha_N}}}^{m_j}\left[\frac{1}{1+sP_jA_{er}h_j^m x^{-(\alpha_N+m)}}\right]^{E\left[n_j^N\right]} \cdot \frac{2x}{m_j^2-\left(\frac{P_j}{P_k}\right)^{\frac{2}{m+\alpha_N}}\left(\frac{h_j}{h_k}\right)^{\frac{2m}{m+\alpha_N}}R^{\frac{2(m+\alpha_L)}{m+\alpha_N}}}dx,\end{aligned} \tag{45}$$

where $U_{N,j}^L$ is the set of interfering UAVs implementing NLoS transmission in tier j. Substituting (44) and (45) into (43), we can obtain (40), which completes the proof. ■

Similarly, given that the serving ABS with NLoS transmission has distance R, the Laplace transform of the interference power, $I_L + I_N$, is

$$\mathcal{L}_I^N\left(s|R\right) = \mathbb{E}_{I_L}^N\left[\exp\left(-sI_L\right)|R\right]\mathbb{E}_{I_N}^N\left[\exp\left(-sI_N\right)|R\right], \tag{46}$$

where

$$\mathbb{E}_{I_L}^{N}\left[\exp\left(-sI_L\right)|R\right] = \prod_{j=1}^{K}\int_{\left(\frac{P_j}{P_k}\right)^{\frac{1}{m+\alpha_L}}\left(\frac{h_j}{h_k}\right)^{\frac{m}{m+\alpha_L}}R^{\frac{m+\alpha_N}{m+\alpha_L}}}^{m_j}\left(1+\frac{sP_jA_{er}h_j^m x^{-\alpha_L-m}}{m_0}\right)^{-m_0\mathbb{E}\left[n_j^L\right]} \cdot \frac{2x}{m_j^2-R^{\frac{2(m+\alpha_N)}{m+\alpha_L}}\left(\frac{P_j}{P_k}\right)^{\frac{2}{m+\alpha_L}}\left(\frac{h_j}{h_k}\right)^{\frac{2m}{m+\alpha_L}}}dx, \tag{47}$$

and

$$\mathbb{E}_{I_N}^{N}\left[\exp\left(-sI_N\right)|R\right] = \prod_{j=1,j\neq k}^{K}\cdot\int_{\left(\frac{P_j}{P_k}\right)^{\frac{1}{m+\alpha_N}}\left(\frac{h_j}{h_k}\right)^{\frac{m}{m+\alpha_N}}R}^{m_j}\left(\frac{1}{1+sP_jA_{er}h_j^m x^{-(\alpha_N+m)}}\right)^{\mathbb{E}\left[n_j^N\right]} \frac{2x}{m_j^2-R^2\left(\frac{P_j}{P_k}\right)^{\frac{2}{m+\alpha_N}}\left(\frac{h_j}{h_k}\right)^{\frac{2m}{m+\alpha_N}}}dx \cdot \int_{R}^{m_k}\left(\frac{1}{1+sP_kA_{er}h_j^m x^{-(\alpha_N+m)}}\right)^{\left(\mathbb{E}\left[n_k^N\right]-1\right)}\frac{2x}{m_k^2-R^2}dx. \tag{48}$$

Based on(40) and (46), the coverage probability of the K-tier UAV networks can be obtained in the following theorem.

Theorem 3: The total coverage probability of the K-tier UAV network, defined as $P_c = \sum_{k=1}^{n}\left(\mathbb{P}^L(A=k)A_k^L + \mathbb{P}^N(A=k)A_k^N\right)$, cf. (37), can be obtained by substituting

$$\mathbb{P}^L(A=k) = \sum_{i=1}^{m_0}(-1)^{i+1}\binom{m_0}{i}\int_{h_k}^{m_k}\mathcal{L}_I^L\left(s\right)|_{s=M}f_{R_k^L|A_k^L}(r)\mathrm{d}r, \tag{49}$$

and

$$\mathbb{P}^N(A=k) = \int_{h_k}^{m_k}\mathcal{L}_I^N\left(s\right)|_{s=P_k^{-1}A_{er}^{-1}h_k^{-m}R_{k,o}^{\alpha_L+m}T}f_{R_k^L|A_k^L}(r)\mathrm{d}r. \tag{50}$$

where $M = i\eta P_k^{-1}A_{er}^{-1}h_k^{-m}R_{k,o}^{\alpha_L+m}T$. Moreover, A_k^L and A_k^N are given in (22) and (25), respectively.

Proof: The coverage probability of the typical UE associated with the serving ABS under LoS transmission in tier k can be calculated as

$$\begin{aligned}\mathbb{P}^L(A=k) &= \mathbb{E}_{R_{k,o}}\left[\mathbb{P}\left\{\mathrm{SIR}_k^L\left(R_{k,o}\right)\geq \mathrm{T}\right\}\right] \\ &= \int_{h_k}^{m_k}\mathbb{P}\left\{\mathrm{SIR}_k^L(r)\geq \mathrm{T}\right\}f_{R_k^L}(r)\mathrm{d}r.\end{aligned} \tag{51}$$

$$
\begin{aligned}
&\mathbb{E}_{I_L}^{L}\left[\exp\left(-sI_L\right)|R\right]\\
&=\mathbb{E}_{I_L}\left[\exp\left(-s\left(\sum_{j=1,j\neq k}^{K}\sum_{i=1}^{E\left[n_j^L\right]}I_{i,j}+\sum_{i=1}^{E\left[n_k^L\right]-1}I_{i,k}\right)\right)|R\right]\\
&=\mathbb{E}_{I_L}\left[\prod_{j=1,j\neq k}^{K}\prod_{i=1}^{E\left[n_j^L\right]}\exp\left(-sP_jA_{er}\left(\frac{h_j}{u_{i,j}}\right)^{m}G_{u_{ij}}u_{i,j}^{-\alpha_L}\right)\cdot\prod_{i=1}^{E\left[n_k^L\right]-1}\exp\left(-sP_kA_{er}\left(\frac{h_k}{u_{i,j}}\right)^{m}G_{u_{i,k}}u_{i,k}^{-\alpha_L}\right)|R\right]\\
&=\prod_{j=1,j\neq k}^{K}\mathbb{E}_{U_j^L,G_j^L}\left[\prod_{i=1}^{E\left[n_j^L\right]}\exp\left(-sP_jA_{er}h_j^mG_{u_{i,j}}u_{i,j}^{-(\alpha_L+m)}\right)|R\right]\cdot\mathbb{E}_{U_k^L,G_k^L}\left[\prod_{i=1}^{E\left[n_k^L\right]-1}\exp\left(-sP_kA_{er}h_k^mG_{u_{i,j}}u_{i,k}^{-(\alpha_L+m)}\right)|R\right]\\
&=\prod_{j=1,j\neq k}^{K}\mathbb{E}_{U_j^L}\left[\prod_{i=1}^{E\left[n_j^L\right]}\mathbb{E}_G\left[\exp\left(-SP_jA_{er}h_j^mGu_{i,j}^{-(\alpha_L+m)}\right)\right]|R\right]\cdot\mathbb{E}_{U_k^L}\left[\prod_{i=1}^{E\left[n_k^L\right]-1}\mathbb{E}_G\left[\exp\left(-SP_kA_{er}h_k^mGu_{i,k}^{-(\alpha_L+m)}\right)\right]|R\right]\\
&=\prod_{j=1,j\neq k}^{K}\mathbb{E}_{U_j^L}\left[\left[\left(1+\frac{sP_jA_{er}h_j^mu_{i,j}^{-(\alpha_L+m)}}{m_0}\right)^{-m_0}|R\right]^{E\left[n_j^L\right]}\right]\mathbb{E}_{U_k^L}\left[\left[\left(1+\frac{sP_kA_{er}h_k^mu_{i,k}^{-(\alpha_L+m)}}{m_0}\right)^{-m_0}|R\right]^{E\left[n_k^L\right]-1}\right]\\
&=\prod_{j=1,j\neq k}^{K}\int_{\left(\frac{P_j}{P_k}\right)^{\frac{1}{m+\alpha_L}}\left(\frac{h_j}{h_k}\right)^{\frac{m}{m+\alpha_L}}R}^{m_j}\left[\left(1+\frac{sP_{\max}A_{er}h_j^mx^{-(\alpha_L+m)}}{m_0}\right)^{-m_0}\right]^{E\left[n_j^L\right]}\frac{2x}{m_j^2-\left(\frac{P_j}{P_k}\right)^{\frac{2}{m+\alpha_L}}\left(\frac{h_j}{h_k}\right)^{\frac{2m}{m+\alpha_L}}R^2}dx\\
&\cdot\int_{R}^{m_k}\left[\left(1+\frac{sP_{\max}A_{er}h_j^mx^{-(\alpha_L+m)}}{m_0}\right)^{-m_0}\right]^{E\left[n_k^L\right]-1}\frac{2x}{m_k^2-R^2}dx.
\end{aligned}
\tag{44}
$$

where $f_{R_k^L}(r)$ is given in Lemma 3. Moreover, we have

$$
\begin{aligned}
&\mathbb{P}\left\{\mathrm{SIR}_k^L\left(R_{k,o}\right)\geq T\right\}\\
&=\mathbb{P}\left\{G_{r_{k,o}}\geq P_k^{-1}A_{er}^{-1}h_k^{-m}R_{k,o}^{\alpha_L+m}T\left(I_L+I_N\right)\right\}\\
&\overset{(a)}{\approx}1-\mathbb{E}_I\left[\left[1-\exp\left(-\eta P_k^{-1}A_{er}^{-1}h_k^{-m}R_{k,o}^{\alpha_L+m}T(I_L+I_N)\right)\right]^{m_0}\right]\\
&=\sum_{i=1}^{m_0}\binom{m_0}{i}(-1)^{i+1}\mathbb{E}_I\left[\exp(-sI)\right]_{s=i\eta P_k^{-1}A_k^{-1}h_k^{-m}R_{k,o}^{\alpha_L+m}T}.
\end{aligned}
\tag{52}
$$

where (a) follows from Lemma 6 in [34] and $\eta = m_0\left(m_0!\right)^{(1/m_0)}$. Similarly, we have

$$
\begin{aligned}
&\mathbb{P}\left\{\mathrm{SIR}_k^N\left(R_{k,o}\right)\geq T\right\}\\
&=\mathbb{P}\left\{H_{r_{k,o}}\geq P_k^{-1}A_{er}^{-1}h_k^{-m}R_{k,o}^{\alpha_L+m}T\left(I_L+I_N\right)\right\}\\
&=\mathbb{E}_I\left[\exp\left(-P_k^{-1}A_{er}^{-1}h_k^{-m}R_{k,o}^{\alpha_L+m}T\left(I_L+I_N\right)\right)\right]\\
&=\mathbb{E}_I\left[\exp(-sI)\right]\big|_{s=P_k^{-1}A_{er}^{-1}h_k^{-m}R_{k,o}^{\alpha_L+m}T}.
\end{aligned}
\tag{53}
$$

Based on Lemma 5 and (46), Theorem 3 can be thus proved. ■

VI. NUMERICAL AND SIMULATION RESULTS

In this section, we evaluate the performance of a two-tier UAV network, where the ABSs in tier 1 and 2 are located at heights h_1 and h_2, respectively. Unless otherwise specified, the simulation parameters are set according to Table II. We present both analytical and simulation results, where Monte Carlo simulations are employed to validate the analytical results obtained in Sections III-V. Thereby, the horizontal locations of UAVs and UEs are randomly generated in a large plane and the height of UAVs in each tier is set based on the empirical data from Qualcomm [35]. We simulate 10^4 spatial realizations for the locations of ground UEs and UAVs. For each spatial realization, the locations of the ground UEs and UAVs are fixed, which enables us to obtain the empirical connection and coverage probabilities. The final results are gathered by averaging over all simulation realizations. We note that Monte Carlo simulations have been widely adopted to evaluate performance and validate analytical derivation for cellular networks and UAV networks [29], [36], [37].

A. CONNECTION PROBABILITY OF THE UAV NETWORK

Fig. 4 shows the connection probability of the considered UAV network as a function of the height of the first-tier ABSs when different receiving thresholds are employed at the ground UEs. From Fig. 4 we observe that the Monto Carlo simulation results are in a good match with the analytical results, implying that the derivations in Section III are valid. As the height of the first-tier ABSs increases in the small value regime, the connection probability increases quickly before it saturates. This result is due to the high directivity of

TABLE 2. SIMULATION PARAMETERS

Parameter	Default Value
$P_{\max}$	1W
ρ_c	$-50dBm$
α_L	2
α_N	2.8
h_1	$100m$ [35]
h_2	$2h_1$ [35]
λ_1	$10/km^2$
λ_2	λ_1
m_0	3
m	6
T	0.1
A_{er}	5dB

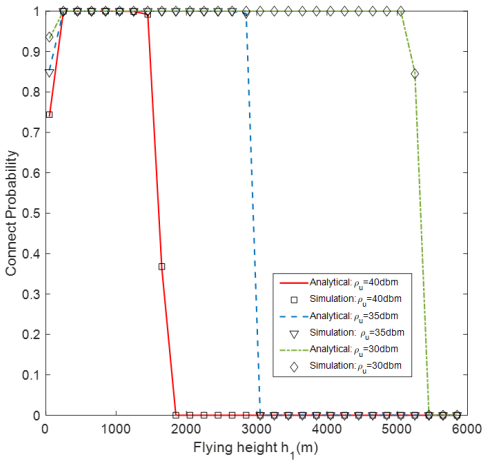

FIGURE 4. Connection probability of the UAV network versus flying height of the first-tier ABSs for different receiving thresholds of the ground UEs.

directional antenna. In particular, the ABSs at a low height would transmit signal over the sidelobe of the generated beam, resulting in only small antenna gain. In this case, the connection probability of the UAV network is small. As the ABSs's height increases, the connection probability of the UAV networks improve as more UEs receive signal from the main lobe of the UAVs such that the associated antenna gain increases. On the other hand, we also observe from Fig. 4 that, after the flying height exceeds a limit, e.g., 1300 m for receiving threshold ρ_u=40 dBm, the connection probability quickly drops to zero. This is consistent with our derivations of the maximum flying height in Section III. In particular, due to the receiving threshold of the typical UE and the maximum output power of the ABSs, only ABSs within a given flying height can activate the receiving circuit at the UEs. Consequently, the region where ABSs can overcome the path loss to a UE shrinks when the height of the ABSs increases and further vanishes when the flying height of the ABSs exceeds $h^L_{\max}$. In the latter case, the connection probability of the UAV network decreases quickly.

Fig. 5 evaluates the connection probability of the consid-

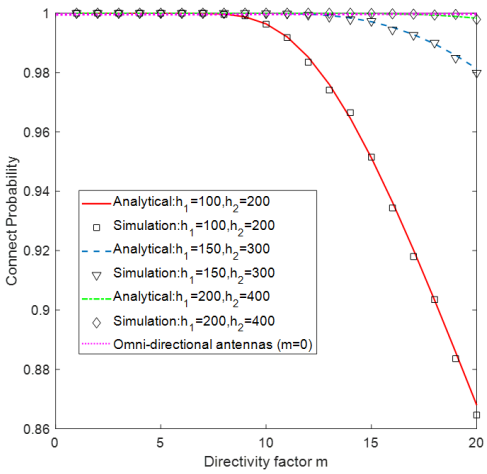

FIGURE 5. Connection probability versus directivity factor of antenna element for different flying heights of the ABSs.

ered UAV network as a function of the antenna's directivity factor when the ABSs adopt different flying heights. From Fig. 5 we observed that, for directional antennas, the connection probability decreases with the antenna's directivity factor. This is because the main lobe of the generated directional beam shrinks as the directivity factor increases. Consequently, a UE has to communicate with the ABS via the side lobe with a high probability, which reduces the connection probability. In contrast, for omni-directional antennas with m=0, the connection probability is always close to 1 for the considered simulation setup. Moreover, by employing directional antenna, it is interesting to observe that the ABSs flying at a large height can provide a high connection probability, espcially when the directivity factor is large. This is because, as the flying height increases, only the ABSs close to the top of their served UEs can successfully connect with the UEs. Although a high directivity factor leads to a disc of small the radius, the large antenna gain enables ABSs to connect with the UE at large height. This result implies that the UAV network employing highly directive antennas is suitable to fly at a large height provided it is within the limit of the flying maximum height.

Fig. 6 shows the connectivity probability as a function of the receiving threshold when the UAVs employ antennas of different directivity factors. From Fig. 6 we observe that the connection probability of the considered UAV network decreases with the receiving threshold of the UE. However, as the directivity factor of antenna elements increases, the connection probability tends to decrease with the receiving threshold at a slower rate. This is because the radius of the disc decreases with the directivity factor; consequently, fewer ABSs can successfully connect with the ground UEs using their transmit output power. In the large regime of the receiving threshold, the connection probability of UAV

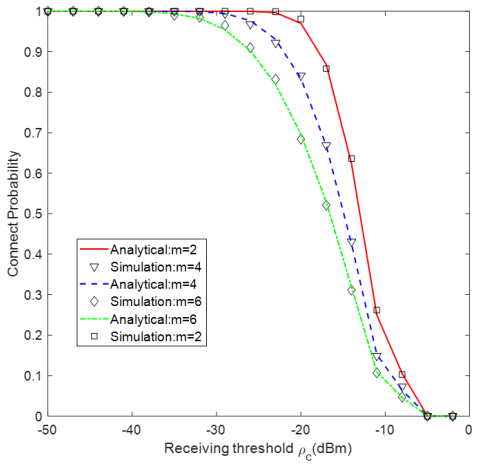

FIGURE 6. Connection probability versus receiving threshold of the ground UEs for antennas of different directivity factors.

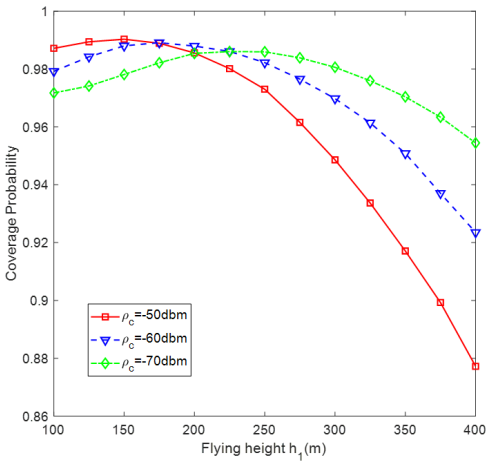

FIGURE 7. Coverage probability versus flying height of the first-tier ABSs for different received thresholds of the ground UEs.

network decreses sharply and approaches 0. In the latter case, the ground UE cannot connect to the UAV network. This is because the maximal transmission height decreases with the receiving threshold. Consequently, more ABSs at large flying heights will fail in signal transmission until, when the receiving threshold of ground UEs is large enough, none of the ABSs can successfully connect with the ground UEs.

B. COVERAGE PROBABILITY OF THE UAV NETWORK

Fig. 7 shows the total coverage probability as a function of the flying height of the first-tier ABSs when the ground UEs employ different receiving thresholds. From Fig. 7 we observe that there exists an optimal flying height that achieves the maximal coverage probability. This is because by employing directional antennas, the radius of disc b_k increases with the height of the ABSs such that more ABSs can serve the UEs. When the flying height of the ABSs is low (e.g. $100\,\text{m} < h_1 < 200\,\text{m}$), the radius of the disc is small such that few ABSs can successfully activate the ground UE. As the flying height of the ABSs increases, the disc of radius as well as the connection probability of the UAV network improves. Nevertheless, as the number of interfering ABSs also increases with the radius of the disc, the coverage probability deteriorates. Therefore, a tradeoff between the connection probability and the coverage probability exists when employing directional antenna in UAV networks and the maximal coverage probability of the UAV networks is achieved at the optimal flying height by balancing between signal enhancement and interference mitigation. From Fig. 7 we also observed that the coverage probability decreases quickly for large receiving thresholds of the ground UEs. This is because, by adopting large receiving thresholds, the distances between the ground UEs and their serving ABSs decrease. Consequently, the ABSs at a large flying height have to overcome the large path loss, which reduces the

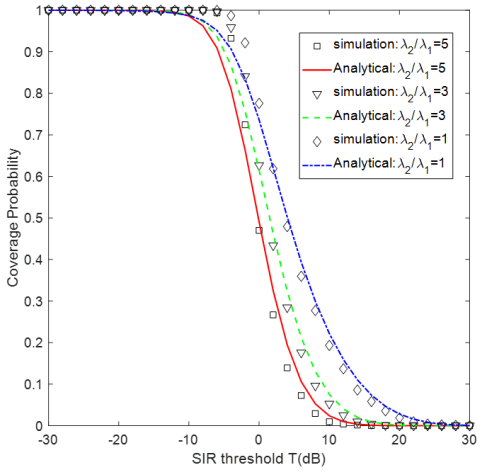

FIGURE 8. Coverage probability versus SIR threshold of the UAV networks for different densities of the ABSs.

coverage probability of the UAV network.

Fig. 8 shows the coverage probability as a function of the SIR threshold for different densities of UAVs. From Fig. 8, we observe that the coverage probability decreases with the SIR threshold. Similar results for a two-tier terrestrial cellular network have been reported in [38]. We note that, in the same SIR threshold regime, the coverage probability of the considered two-tier UAV network is always larger than that of the two-tier cellular network considered in [38]. This is because the directional antenna provides additional antenna gains to overcome the path loss and, at the same time, reduce the impact of interfering ABSs. Moreover, as the density of the ABSs increases, the coverage probability decreases due to the increased number of interfering ABSs.

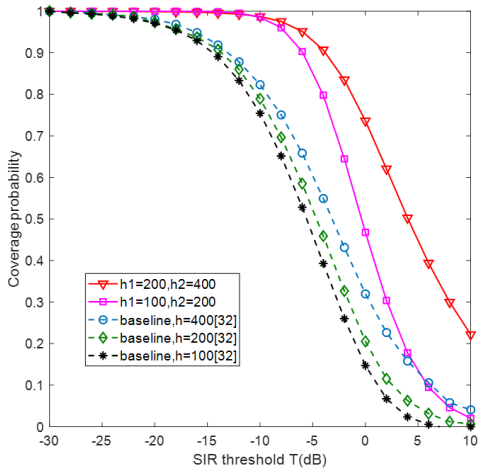

FIGURE 9. Coverage probability versus SIR threshold of the UAV network for different heights of the ABSs.

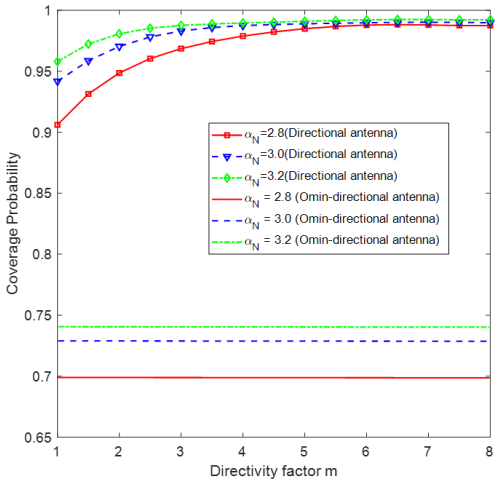

FIGURE 10. Coverage probability versus directivity factor of directional antenna for different path loss exponents of NLoS transmission.

Fig. 9 compares the coverage probability of the considered two-tier UAV network with the baseline one-tier UAV network as considered in [28]. For both networks, the coverage probability is evaluated as a function of the SIR threshold for deploying the UAVs at different flight heights, where the path loss exponent is $\alpha_N = 2.5$. It can be seen from Fig. 9 that the coverage probabilities of the considered UAV networks shows the same tendency, which decreases with the SIR threshold. However, the proposed two-tier UAV network with directional antenna always outperform the baseline UAV network for the considered SIR thresholds.

Finally, Fig. 10 shows the coverage probability as a function of the antenna's directivity factor for different path loss exponents under NLoS transmission. From Fig. 10 we observe that, for directional antennas, the coverage probability increases with the antenna's directivity factor, as the antenna gain of the serving ABSs enlarges. When the directivity factor is high enough, the radius of the disc reduces. In this case, both the serving ABS and the interfering ABSs are located close to the center of the disc and the number of interfering ABSs reduces. Consequently, the SIR increases with the directivity factor of antennas and application of directional antennas leads to much higher coverage probability than that of omni-directional antennas. From Fig. 10 we also observe that, with a large pass loss exponent, the UAV network can obtain a high coverage probability. This result implies that UAVs equipped with directional antenna can achieve high coverage probability even for propagation scenarios of large path loss.

VII. CONCLUSIONS AND FUTURE WORK

This paper developed a novel analytical framework for evaluating the distance distribution, connectivity probability, and coverage probability of K-tier UAV networks that employ directional antennas. To facilitate a tractable performance analysis, we introduced a simple elevation angle based antenna pattern model to capture the antenna gain provided by directional antennas. It was revealed that the directivity factor can highly impact the connection probability, especially when the UAVs deployed at low flying heights have a large elevation angle. However, the coverage probability of K-tier UAV networks can be enhanced by adopting directional antennas as the interference power caused from other ABSs reduced. Both the analytical and simulation results showed that the application of directional antennas for UAVs at large flying heights can provide excess antenna gain to overcome the propagation pass loss and, at the same time, mitigate the impact of interfering UAVs. These results demonstrated the huge potential of employing directional antennas to enhance the performance of multi-tier UAV networks. In the future, the application of directional antenna for uplink communication and the associated performance evaluation of multi-tier UAV networks in the uplink are interesting extensions of this work. Moreover, selecting the optimal directivity factor of directional antennas for given density and flying height of UAVs is another compelling research direction.

REFERENCES

[1] Y. Zeng, R. Zhang, and T. J. Lim, "Wireless communications with unmanned aerial vehicles: opportunities and challenges," IEEE Communication Magazine, vol. 54, no. 5, pp. 36–42, May 2016.
[2] M. Mozaffari, W. Saad, M. Bennis, Y. Nam, and M. Debbah, "A tutorial on uavs for wireless networks: Applications, challenges, and open problems," IEEE Communications Surveys Tutorials, pp. 1–1, 2019.
[3] 3GPP Technical Report 36.777. Technical specification group radio access network; Study on enhanced LTE support for aerial vehicles (Release 15). Dec. 2017.
[4] "Paving the path to 5G: Optimizing commercial lte networks for drone communication," available online: https://www.qualcomm.com/news/onq/2016/09/06/paving-path-5goptimizing-commercial-lte-networks-drone-communication.

[5] A. Fotouhi, H. Qiang, M. Ding, M. Hassan, L. G. Giordano, A. Garcia-Rodriguez, and J. Yuan, "Survey on UAV cellular communications: Practical aspects, standardization advancements, regulation, and security challenges," IEEE Communications Surveys Tutorials, pp. 1–1, 2019.
[6] A. E. A. A. Abdulla, Z. M. Fadlullah, H. Nishiyama, N. Kato, F. Ono, and R. Miura, "An optimal data collection technique for improved utility in uas-aided networks," Proc. IEEE INFOCOM, pp. 736–744, April 2014.
[7] H. Kim and J. Ben-Othman, "A collision-free surveillance system using smart UAVs in multi domain IoT," IEEE Communications Letters, vol. 22, no. 12, pp. 2587–2590, December 2018.
[8] N. Zhao, W. Lu, M. Sheng, Y. Chen, J. Tang, F. R. Yu, and K. Wong, "UAV-assisted emergency networks in disasters," IEEE Wireless Communications, vol. 26, no. 1, pp. 45–51, February 2019.
[9] M. Alzenad, A. El-Keyi, and H. Yanikomeroglu, "3-D placement of an unmanned aerial vehicle base station for maximum coverage of users with different QoS requirements," IEEE Wireless Communications Letters, vol. 7, no. 1, pp. 38–41, February 2018.
[10] X. Wang, H. Zhang, Y. Tian, and V. C. M. Leung, "Modeling and analysis of aerial base station-assisted cellular networks in finite areas under los and nlos propagation," IEEE Transactions on Wireless Communications, vol. 17, no. 10, pp. 6985–7000, October 2018.
[11] A. V. Savkin and H. Huang, "Deployment of unmanned aerial vehicle base stations for optimal quality of coverage," IEEE Wireless Communications Letters, vol. 8, no. 1, pp. 321–324, February 2019.
[12] H. He, S. Zhang, Y. Zeng, and R. Zhang, "Joint altitude and beamwidth optimization for UAV-enabled multiuser communications," IEEE Communications Letters, vol. 22, no. 2, pp. 344–347, February 2018.
[13] J. Chen, J. Xie, Y. Gu, S. Li, S. Fu, Y. Wan, and K. Lu, "Long-range and broadband aerial communication using directional antennas (ACDA): Design and implementation," IEEE Transactions on Vehicular Technology, vol. 66, no. 12, pp. 10 793–10 805, December 2017.
[14] D. He, T. Bouras, X. Chen, W. Yu, Y. Zhang, and Y. Yang, "3-D spatial spectrum fusion indoor localization algorithm based on CSI-UCA smoothing technique," IEEE Access, vol. 6, pp. 59 575–59 558, 2018.
[15] A. Abdelreheem, E. M. Mohamed, and H. Esmaiel, "Location-based millimeter wave multi-level beamforming using compressive sensing," IEEE Communications Letters, vol. 22, no. 1, pp. 185–188, Jane 2018.
[16] A. Abdelreheem, E. M. Mohamed, and H. Esmaiel, "Adaptive location-based millimetre wave beamforming using compressive sensing based channel estimation," IET Communications, vol. 13, no. 9, pp. 1287–1296, 2019.
[17] I. Bor-Yaliniz and H. Yanikomeroglu, "The new frontier in RAN heterogeneity: Multi-tier drone-cells," IEEE Communications Magazine, vol. 54, no. 11, pp. 48–55, November 2016.
[18] S.Sekander, H.Tabassum, and E.Hossain, "Multi-tier drone architecture for 5G/B5G cellular networks: Challenges, trends, and prospects," IEEE Communications Magazine, vol. 56, no. 3, pp. 96–103, March 2018.
[19] D. Kim, J. Lee, and T. Q. S. Quek, "Multi-layer unmanned aerial vehicle networks: Modeling and performance analysis," arXiV:1904.01167v1.
[20] K. Venugopal, M. C. Valenti, and R. W. Heath, "Device-to-device millimeter wave communications: Interference, coverage, rate, and finite topologies," IEEE Transactions on Wireless Communications, vol. 15, no. 9, pp. 6175–6188, September. 2016.
[21] M. M. Selim, M. Rihan, Y. Yang, L. Huang, Z. Quan, and J. Ma, "On the outage probability and power control of D2D underlaying noma uav-assisted networks," IEEE Access, vol. 7, pp. 16 525–16 536, 2019.
[22] J. Wang, C. Jiang, Z. Wei, C. Pan, H. Zhang, and Y. Ren, "Joint uav hovering altitude and power control for space-air-ground iot networks," IEEE Internet of Things Journal, vol. 6, no. 2, pp. 1741–1753, April 2019.
[23] G. Zhang, Q. Wu, M. Cui, and R. Zhang, "Securing uav communications via joint trajectory and power control," IEEE Transactions on Wireless Communications, vol. 18, no. 2, pp. 1376–1389, Feb. 2019.
[24] J. Zhang, L. Xiang, D. W. K. Ng, M. Jo, and M. Chen, "Energy efficiency evaluation of multi-tier cellular uplink transmission under maximum power constraint," IEEE Transactions on Wireless Communications, vol. 16, no. 11, pp. 7092–7107, November 2017.
[25] T. Hou, Y. Liu, Z. Song, X. Sun, and Y. Chen, "Multiple antenna aided NOMA in UAV networks: A stochastic geometry approach," IEEE Transactions on Communications, vol. 67, no. 2, pp. 1031–1044, Feb. 2019.
[26] J. Kim, J. Park, S. Kim, S. Kim, K. W. Sung, and K. S. Kim, "Millimeter-wave interference avoidance via building-aware associations," IEEE Access, vol. 6, pp. 10 618–10 634, 2018.
[27] X. Yu, J. Zhang, M. Haenggi, and K. B. Letaief, "Coverage analysis for millimeter wave networks: The impact of directional antenna arrays," IEEE Journal on Selected Areas in Communications, vol. 35, no. 7, pp. 1498–1512, July 2017.
[28] V. V. Chetlur and H. S. Dhillon, "Downlink coverage analysis for a finite 3-D wireless network of unmanned aerial vehicles," IEEE Transactions on Communications, vol. 65, no. 10, pp. 4543–4558, October 2017.
[29] P. K. Sharma and D. I. Kim, "Random 3D mobile UAV networks: Mobility modeling and coverage probability," IEEE Transactions on Wireless Communications, vol. 18, no. 5, pp. 2527–2538, May 2019.
[30] M. Haenggi, "Stochastic geometry for wireless networks," Cambridge, U.K.: Cambridge Univ. Press, 2013.
[31] Z. Wang, P. S. Hall, J. R. Kelly, and P. Gardner, "Wideband frequency-domain and space-domain pattern reconfigurable circular antenna array," IEEE Transactions on Antennas and Propagation, vol. 65, no. 10, pp. 5179–5189, October 2017.
[32] J. Kraus and R. J. Marthefka, "Antennas: For all applications," McGraw-Hill, New York, 2002.
[33] A. Al-Hourani, S. Kandeepan, and S. Lardner, "Optimal LAP altitude for maximum coverage," IEEE Wireless Communications Letters, vol. 3, no. 6, pp. 569–572, December 2014.
[34] T. Bai and R. W. Heath, "Coverage and rate analysis for millimeter-wave cellular networks," IEEE Transactions on Wireless Communications, vol. 14, no. 2, pp. 1100–1114, February 2015.
[35] Qualcomm, LTE Unmanned Aircraft SystemsąTrial Report, vol. Qualcomm Technologies, Inc., May 2017.
[36] V. Naghshin, M. C. Reed, and N. Aboutorab, "Coverage analysis of packet multi-tier networks with asynchronous slots," IEEE Transactions on Communications, vol. 65, no. 1, pp. 200–215, Jan. 2017.
[37] L. Xiang, X. Ge, C. Wang, F. Y. Li, and F. Reichert, "Energy efficiency evaluation of cellular networks based on spatial distributions of traffic load and power consumption," IEEE Transactions on Wireless Communications, vol. 12, no. 3, pp. 961–973, March 2013.
[38] H. Jo, Y. J. Sang, P. Xia, and J. G. Andrews, "Heterogeneous cellular networks with flexible cell association: A comprehensive downlink sinr analysis," IEEE Transactions on Wireless Communications, vol. 11, no. 10, pp. 3484–3495, October 2012.

JING ZHANG received the Ph.D. degree from Huazhong University of Science and Technology (HUST) in 2002 and 2010, respectively. He is currently an associate professor with HUST. His current research interests include unmanned aerial vehicle communications, green communications, device-to-device communications, and millimeter-wave communications.

HUAN XU received his undergraduate degree from Wuhan University of Technology and is currently pursuing a master's degree at Huazhong University of Science and Technology. His current research interests include green communication, stochastic geometry and UAV wireless network performance analysis.

LIN XIANG (S'14, M'18) received the Bachelor and Master degrees in electronics and information engineering from Huazhong University of Science and Technology (HUST), China, in 2009 and 2012, respectively, and the PhD degree from Friedrich-Alexander-University of Erlangen-Nuremberg (FAU), Germany, in 2018. From Aug. 2010 to Feb. 2011, he was an exchange student at University of Bologna, Italy, under support from Erasmus Mundus programme. He is currently a research associate with the Interdisciplinary Centre for Security, Reliability and Trust (SnT), University of Luxembourg, Luxembourg. His research interests include resource allocation for wireless communication systems, performance analysis of wireless networks based on stochastic geometry theory, and renewable energy integration and electric vehicle charging in smart grid. Dr. Xiang was a recipient of the Best Paper Award for IEEE Globecom 2010. He was an Exemplary Reviewer of the IEEE TRANSACTIONS ON WIRELESS COMMUNICATIONS in 2018 and the IEEE TRANSACTIONS ON COMMUNICATIONS in 2017 and 2018.

JUN YANG received Bachelor and Master degree in Software Engineering from Huazhong University of Science and Technology (HUST), China in 2008 and 2011, respectively. Then, he got his Ph.D degree at School of Computer Science and Technology, HUST, on June 2018. Currently, he works as a postdoctoral fellow at Embedded and Pervasive Computing (EPIC) Lab in School of Computer Science and Technology, HUST. His research interests include cognitive computing, software intelligence, Internet of Things, cloud computing and big data analytics, etc.